Ultrafast carrier dynamics in undoped and *p*-doped InAs/GaAs quantum dots characterized by pump-probe reflection measurements

Hai-Ying Liu,[1] Zi-Ming Meng,[1] Qiao-Feng Dai,[1] Li-Jun Wu,[1] Qi Guo,[1] Wei Hu,[1] Song-Hao Liu,[1] Sheng Lan,[1,a)] and Tao Yang[2]
[1]*Laboratory of Photonic Information Technology, School for Information and Optoelectronic Science and Technology, South China Normal University, Guangzhou, Guangdong 510006, People's Republic of China*
[2]*Nano-Optoelectronics Laboratory, Institute of Semiconductors, Chinese Academy of Science, P.O. Box 912, Bejing 100083, People's Republic of China*

(Received 2 November 2007; accepted 28 February 2008; published online 28 April 2008)

We investigate the dependence of the differential reflection on the structure parameters of quantum dot (QD) heterostructures in pump-probe reflection measurements by both numerical simulations based on the finite-difference time-domain technique and theoretical calculations based on the theory of dielectric films. It is revealed that the value and sign of the differential reflection strongly depend on the thickness of the cap layer and the QD layer. In addition, a comparison between the carrier dynamics in undoped and *p*-doped InAs/GaAs QDs is carried out by pump-probe reflection measurements. The carrier capture time from the GaAs barrier into the InAs wetting layer and that from the InAs wetting layer into the InAs QDs are extracted by appropriately fitting differential reflection spectra. Moreover, the dependence of the carrier dynamics on the injected carrier density is identified. A detailed analysis of the carrier dynamics in the undoped and *p*-doped QDs based on the differential reflection spectra is presented, and its difference with that derived from the time-resolved photoluminescence is discussed. © *2008 American Institute of Physics*. [DOI: 10.1063/1.2913316]

I. INTRODUCTION

Since the pioneering work of Arakawa and Sakaki in 1982,[1] the physical properties of semiconductor quantum dots (QDs) have been extensively studied due to their potential application in optoelectronic devices for the future.[2] In particular, $In_xGa_{1-x}As/GaAs$ QDs self-organized by Stranski–Kranstanov (SK) growth mode have received intensive studies because their operating wavelength can be designed at 1.3 μm, which is an important wavelength for telecommunication. Accordingly, much effort has been devoted to the investigation of the carrier dynamics in self-organized QDs that may significantly affect the performance of QD-based devices. In general, the carrier dynamics in self-organized QDs include the capture of photogenerated carriers from the barrier and/or the wetting layer into QDs,[3–7] the relaxation of carriers within QDs from the excited states to the ground state,[8–12] and finally the recombination of carriers in QDs.[13–15] While in quantum wells, fast carrier capture and relaxation are mediated by the carrier-phonon interaction, the carrier relaxation in QDs via phonon scattering is highly improbable due to the discrete energy levels in QDs. Thus, the capture and relaxation processes have always been the focus of the carrier dynamics studies in QDs.[16–19] In addition, appropriate doping of QDs is necessary for making QD infrared photodetectors, and a significant improvement in the modulation speed of QD lasers can be achieved by doping QDs.[20–27] Therefore, the influence of doping on the carrier dynamics in QDs is an important issue that needs to be clarified.

To date, ultrafast optical techniques that are commonly used for the characterization of the carrier dynamics in QDs can be classified into two categories. They rely either on the detection of transient photoluminescence[28–31] (PL) or on the measurement of differential transmission or reflection by pump-probe techniques.[4,32–34] In comparison, both methods have their own advantages and limitations. The time-resolved PL measurements provide the information of carrier capture and relaxation to the ground states of QDs. However, clear PL signals can only be obtained at low temperatures, making the experimental setup complicated. On the contrary, the pump-probe measurements can be carried out at room temperature, offering good signal-to-noise ratio. This advantage makes them quite convenient for investigating the carrier dynamics in self-organized QDs. However, there are only a few reports on the pump-probe reflection measurements of QDs partly because the differential reflection spectra of QD heterostructures dominated by carrier dynamics are difficult to interpret as compared to bulk materials.[4,32–34] For a QD heterostructure, although the QD layer sandwiched by the buffer and cap layers is very thin, it plays an important role in determining the reflection of the QD heterostructure. In addition, the cap layer on top of the QD layer also significantly affects the reflection of the QD heterostructure. In the previous reports, the observed differential reflection spectra showed wide variation.[4,32–34] However, no detailed discussion has been presented to address the important issues such as what determines the value and sign of the differential

[a)]Author to whom correspondence should be addressed. Electronic mail: slan@scnu.edu.cn.

 © 2008 American Institute of Physics

reflection signals. Apparently, a QD heterostructure can no longer be simply treated as a bulk material when its reflection is concerned. Therefore, a simple and effective method is needed to analyze the reflection change of QD heterostructures during the carrier capture and relaxation processes. In addition, a comparison of the carrier dynamics between undoped and *p*-doped QDs characterized by pump-probe reflection measurements is still lacking although it has been done by time-resolved PL measurements.

In this article, we present a detailed characterization of undoped and *p*-doped InAs/GaAs QDs by utilizing a degenerate pump-probe reflection measurement. It is organized as follows. In Sec. II, we numerically and theoretically analyze the dependence of the differential reflection on the structure parameters of QD heterostructures based on the finite-difference time-domain (FDTD) technique and the theory of dielectric films.[35] Then, the growth and structure of the self-organized InAs/GaAs QDs used in our studies are described in Sec. III. The pump-probe reflection measurements carried out at different pump powers for the QD samples are presented in Sec. IV. Section V describes how to extract the time constants for different processes by appropriate exponential fits. A discussion about the dependence of the carrier dynamics on the injected carrier density is given in Sec. VI. In Sec. VII, we present a detailed analysis of the carrier dynamics in the undoped and *p*-doped QDs based on the differential reflection spectra and discuss the difference of the relevant information with that provided by the time-resolved PL measurements. Finally, we summarize our research work in Sec. VIII.

II. DEPENDENCE OF THE DIFFERENTIAL REFLECTION ON THE STRUCTURE PARAMETERS OF QD HETEROSTRUCTURES: ANALYSIS BASED ON THE FDTD TECHNIQUE AND THE THEORY OF DIELECTRIC FILMS

As mentioned above, a QD heterostructure cannot be simply treated as a bulk material when analyzing its reflection. Now let us consider a simple model for an InAs/GaAs QD heterostructure which is schematically shown in Fig. 1(a). The InAs QD layer with a refractive index n_2 is sandwiched by the GaAs cap and buffer layers with a refractive index n_1 which is smaller than n_2. It is generally composed of an InAs wetting layer, an InAs QD layer, and maybe an InGaAs strain relaxation layer. In most cases, the thickness of the InAs QD layer (d_2) is much smaller than those of the GaAs cap and buffer layers (d_1 and d_3). In the initial stage of the pump-probe reflection measurements, most carriers are generated in the GaAs cap and buffer layers. In this case, the differential reflection $\Delta R/R$ of the InAs/GaAs QD heterostructure is mainly induced by the refractive index change Δn_1 in the GaAs cap and buffer layers and it can be expressed as follows:[36]

$$\Delta R/R = 4\Delta n_1/(n_1^2 - 1). \tag{1}$$

Here, Δn_1 is determined by the absorption change in the GaAs cap layer $\Delta\alpha_1$ through the Kramers-Kronig relation,[37]

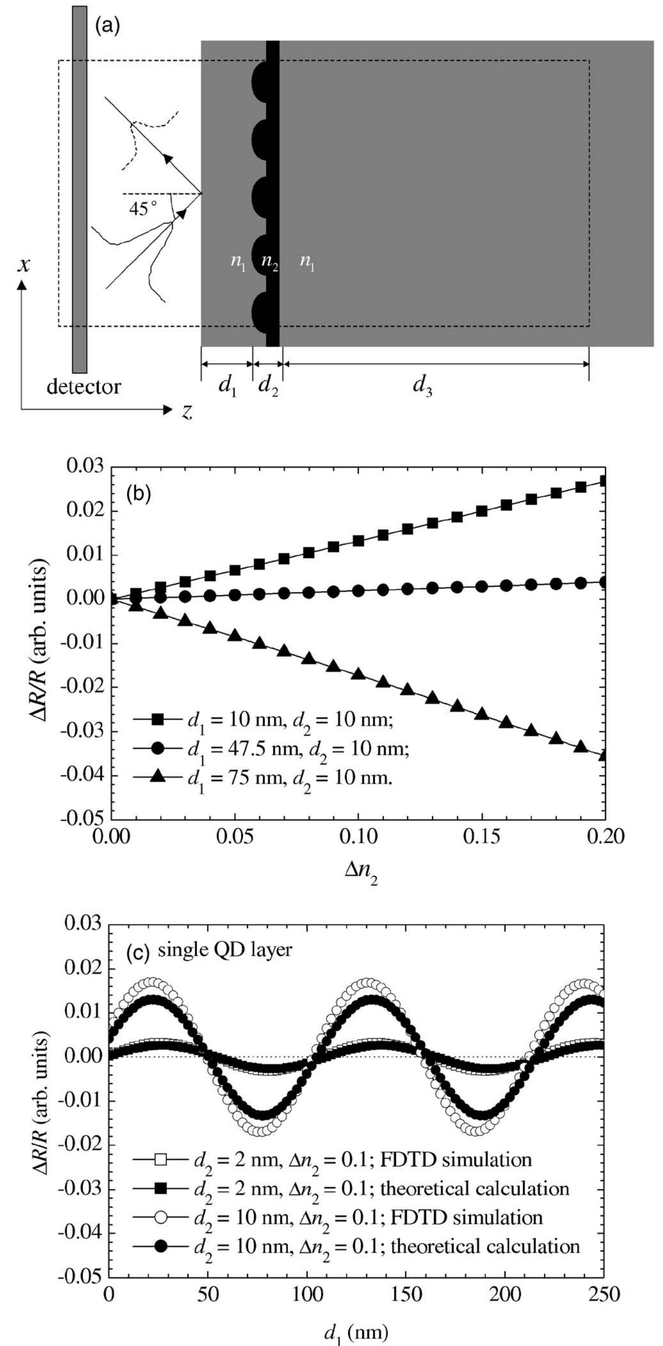

FIG. 1. (a) Schematic of the self-organized QD heterotructure used in FDTD simulations; (b) dependence of the differential reflection on the refractive index change in the QD layer for three QD heterostructures with different cap layers; (c) dependence of the differential reflection on the thickness of the cap layer for two QD heterostructures with different QD layers simulated by the FDTD technique and calculated by the theory of dielectric films.

$$\Delta n_1(E_{\text{probe}},t) \propto P\int_0^\infty \frac{\Delta\alpha_1(E,t)}{E^2 - E_{\text{probe}}^2} dE, \tag{2}$$

where P stands for the principle value of the integral.

With the transfer of the photogenerated carriers from the GaAs barrier to the InAs QD layer, Δn_1 rapidly drops while Δn_2 significantly rises. In this stage, we can neglect temporarily the effect of Δn_1 and try to find out the factor that determines the relationship between $\Delta R/R$ and Δn_2. Since

$\Delta n_2 > 0$, an increase of the reflection would be expected (i.e., $\Delta R > 0$) if the simple bulk material model given above was still applicable. However, it is not true if we carefully examine the dependence of the differential reflection of the QD heterostructure on the thickness of the GaAs cap layer d_1 by FDTD simulation, as will be shown later. For the numerical simulations, the parameters that characterize the structure of the InAs/GaAs QD heterostructure are chosen to be $n_1 = 3.683$, $n_2 = 3.735$, $d_2 = 2$, and 10 nm, $d_3 = 200$ nm, $\Delta n_1 = 0$.[38] The grid sizes along the x and z directions are chosen to be 0.5 and $d_2/10$ nm, respectively. A perfectly matched layer boundary condition is employed for the computation region which is indicated by the dashed box in Fig. 1(a). A Gaussian beam at 800 nm is launched on the sample with an incident angle of 45°, while the power is calculated behind the launch site to record the reflection of the QD heterostructure. For simplicity, we have used continuous waves instead of pulses in the numerical simulations because they enable us to easily calculate the reflection and its dependence on the structure parameters by using the parameter scanning function of the software. No obvious difference is found in the simulation results when pulses are used as incident waves.

In Fig. 1(b), the dependence of $\Delta R/R$ on Δn_2 is plotted for three different values of d_1 when d_2 is fixed to be 10 nm. In all cases, a linear relationship between $\Delta R/R$ and Δn_2 is observed. However, the slope of the linear relationship exhibits a strong dependence on the thickness of the GaAs cap layer d_1. In other words, the value and sign of $\Delta R/R$ are governed by d_1 when d_2 is fixed. For a small value of $d_1 = 10$ nm, we find an increase of $\Delta R/R$ with increasing Δn_2. Since a thin cap layer is generally used in QD heterostructures, a positive $\Delta R/R$ was usually observed in the previous reports.[33] As d_1 is increased to ~ 47.5 nm, $\Delta R/R$ is close to zero and no obvious change is found when Δn_2 is increased. More interestingly, a large decrease of $\Delta R/R$ with increasing Δn_2 is observed when d_1 is further increased to 75 nm. Therefore, it clearly indicates that the QD heterostructure cannot be simply treated as a bulk material although the QD layer is very thin. Its differential reflection exhibits a strong dependence on the thickness of the cap layer.

In order to show more clearly the influence of d_1 and d_2 on R and $\Delta R/R$, we have simulated QD heterostructures with different structure parameters, and some typical results for a fixed $\Delta n_2 = 0.1$ are presented in Fig. 1(c). Apparently, the most remarkable feature is the periodic variation of $\Delta R/R$ with increasing d_1. A careful inspection reveals that the period is approximately given by the half wavelength of the incident light inside the GaAs ($\lambda_1 = 800/n_1$ nm). This phenomenon is easily understood by considering the phase difference between the reflected light from cap layer and that from the QD layer. Since the total reflection is determined by the interference of the reflected light from the cap layer and that from the QD layer, the reflections in case of normal incidence are expected to be the same for two QD heterostructures whose difference in d_1 is equal to $N\lambda_1/2$, where N is an integer. In Fig. 1(c), it is also noticed that the amplitude of the periodic modulation is larger for thicker QD layers. Thus, the periodic modulation of $\Delta R/R$ with increasing d_1 explains the different differential reflection spectra observed in the previous experiments.[4,32–34] Also, it suggests that we can intentionally improve the differential reflection signals by appropriately designing the structure of QD heterostructures, especially the thickness of the cap layer and the QD layer.

Actually, the dependence of the differential reflection of a QD heterostructure on the thickness of the cap layer and the refractive index change of the QD layer can also be theoretically derived. According to the theory of dielectric films,[39–41] the characteristic matrix of a multilayer structure that relates the input and output electric and magnetic fields on either side of the film is given by

$$M_N = \prod_{j=1}^{N} M_j = \prod_{j=1}^{N} \begin{bmatrix} \cos\beta_j & -\frac{i}{p_j}\sin\beta_j \\ -ip_j\sin\beta_j & \cos\beta_j \end{bmatrix}, \qquad (3)$$

where $\beta_j = (2\pi/\lambda_0) n_j d_j \cos\theta_j$ is the phase-shift angle upon traversing the jth layer, p_j is defined as $n_j\cos\theta_j$ and $n_j/\cos\theta_j$ for the s- and p-polarization, d_j is the thickness of the jth layer, and θ_j is the refraction angle.

In our case, a QD heterostructure is considered to be a two-layer structure because the GaAs buffer layer can be regarded as the output medium. Thus, the characteristic matrix for the QD heterostructure can be written as

$$M_2 = \prod_{j=1}^{2} M_j = \begin{bmatrix} m_{11} & m_{12} \\ m_{21} & m_{22} \end{bmatrix} = \begin{bmatrix} \cos\beta_1\cos\beta_2 - \frac{p_2}{p_1}\sin\beta_1\sin\beta_2 & -\frac{i}{p_2}\cos\beta_1\sin\beta_2 - \frac{i}{p_1}\sin\beta_1\cos\beta_2 \\ -ip_1\sin\beta_1\cos\beta_2 - ip_2\cos\beta_1\sin\beta_2 & \cos\beta_1\cos\beta_2 - \frac{p_1}{p_2}\sin\beta_1\sin\beta_2 \end{bmatrix}. \qquad (4)$$

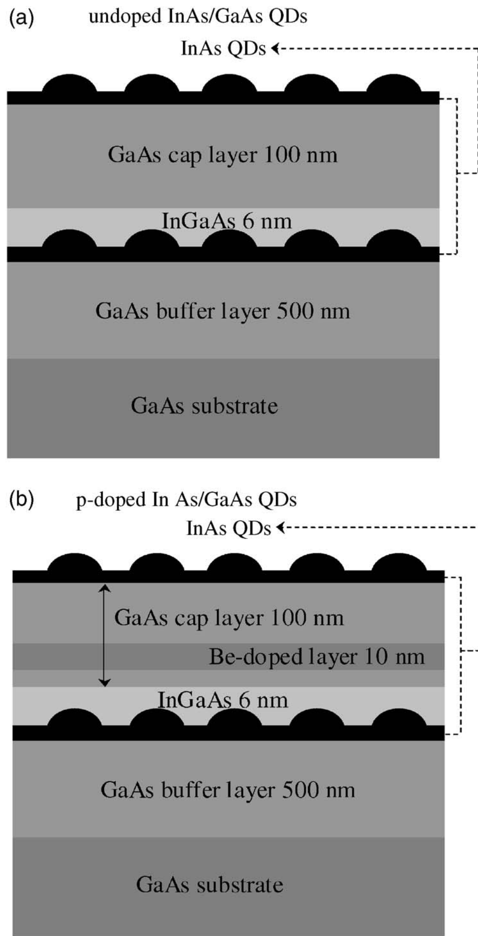

FIG. 2. Schematic structures of the InAs/GaAs QDs (a) undoped and (b) *p*-doped studied in this paper.

Finally, the reflectivity R of the QD heterostructure is derived to be

$$R=\left[\frac{(m_{11}+m_{12}p_3)p_0-(m_{21}+m_{22}p_3)}{(m_{11}+m_{12}p_3)p_0+(m_{21}+m_{22}p_3)}\right]\times\left[\frac{(m_{11}+m_{12}p_3)p_0-(m_{21}+m_{22}p_3)}{(m_{11}+m_{12}p_3)p_0+(m_{21}+m_{22}p_3)}\right]^*, \tag{5}$$

where p_0 and p_3 are the p_j parameters in air and the GaAs buffer layer, respectively.

The dependence of $\Delta R/R$ on d_1 and Δn can be calculated by Eq. (5) and the results are also presented in Fig. 1(c) for comparison. It can be seen that a good agreement is achieved between the theoretical calculation and numerical simulation results. The small discrepancy is attributed to the accuracy of the FDTD simulations that are limited by the grid size. A further reduction of grid size will result in smaller discrepancy.

III. STRUCTURE OF THE UNDOPED AND *P*-DOPED INAS/GAAS QDS

The structures of the undoped and *p*-doped InAs/GaAs QDs studied in this paper are schematically illustrated in Figs. 2(a) and 2(b). They were grown by molecular beam epitaxy. For each sample, the InAs QDs were self-organized by the SK growth mode on a 500 nm GaAs buffer at 500 °C.

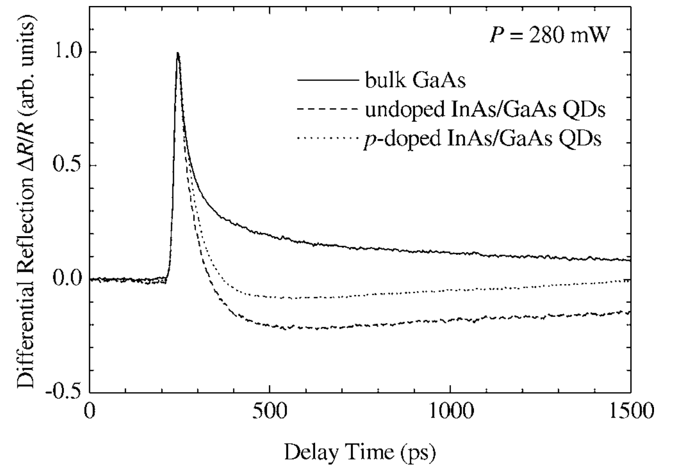

FIG. 3. Differential reflection spectra obtained by pump-probe reflection measurements at a pump power of 280 mW for the bulk GaAs (solid curve), the undoped InAs/GaAs QDs (dashed curve), and the *p*-doped InAs/GaAs QDs (dotted curve).

Then, they were covered by a 6 nm InGaAs strain relax layer followed by a 100 nm GaAs cap layer. On top of the GaAs cap layer, another layer of InAs QDs was deposited under the same growth condition for the atomic force microscope (AFM) observation. The AFM images show that the diameter of the InAs QDs is ~30 nm, while their height is 5–6 nm. The area density of the QDs was estimated to be 4×10^{10} cm^{-2}. For the *p*-doped QDs, a 10 nm Be-doped GaAs layer was inserted into the 100 nm GaAs cap layer. The doping density was chosen to be 10^{18} cm^{-3} and it corresponds to ~10 holes per QD.

IV. PUMP-PROBE REFLECTION MEASUREMENTS FOR THE UNDOPED AND *P*-DOPED INAS/GAAS QDS

The pump-probe reflection measurements were carried out at room temperature by a Ti:sapphire oscillator pumped with a solid state laser (Mira 900, Coherent Company). The width and the repetition rate of the pulse are 130 fs and 76 MHz. The wavelength of the pump and probe pulses was set to be 800 nm, which is about 130 meV above the GaAs absorption edge. The pump and probe beams were focused to spots of 150 and 50 μm in diameter, and they are incident on the sample surface at angles of 0 and 45°, respectively. The time delay between them was provided by a delay line with a minimum step of 3 μm, which corresponds to a time resolution of ~20 fs. In order to find out the effect of the carrier density on the carrier dynamics, the average power of the probe beam was fixed at 6 mW, while that for the pump beam was varied from 60 to 280 mW.

Figure 3 shows the differential reflection spectra obtained at a pump power of 280 mW for the bulk GaAs, the undoped, and *p*-doped InAs/GaAs QDs. The spectra are normalized in order to make a clear comparison of the time constants for various processes. For the bulk GaAs, we observe a sharp increase in the differential reflection followed by a fast and a slow decay. These two decay processes have been attributed to the quick thermalization of the photogenerated carriers and their recombination. Their time constants can be readily extracted by a biexponential fitting. The

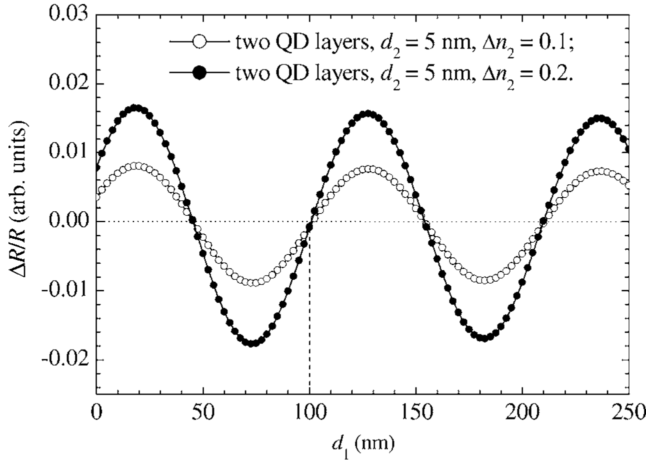

FIG. 4. Simulation results for the dependence of the differential reflection on the thickness of the GaAs cap layer for the QD heterostructure whose structure is similar to those studied in this paper.

longer time constant, which corresponds to the carrier recombination time in bulk GaAs, is extracted to be about 1 ns. It is noticed that ΔR remains to be positive throughout the entire decay process. In comparison, the transient behavior in the differential reflection spectrum is changed for the InAs/GaAs QDs. After a sharp increase in $\Delta R/R$, we can see two fast decay processes with similar time constants followed by a gradually raising process with a much longer time constant. The three stages can be attributed to the capture of the photogenerated carriers from the GaAs barrier into the InAs wetting layer (including the InGaAs strain relaxation layer), the transfer of carriers from the InAs wetting layer (including the InGaAs strain relaxation layer) into the InAs QDs, and the carrier recombination inside the InAs QDs. Obviously, the capture process is much faster than the recombination one. It is remarkable that $\Delta R/R$ becomes negative in the second stage when the carriers are captured into the InAs QDs. This is completely different from that reported in Ref. 33, where $\Delta R/R$ remains to be a positive value. Of course, it is not a surprising result if we have considered that the thickness of the GaAs caper layer and the InAs QD layer are different in our QD samples. We have performed FDTD simulations for the InAs/GaAs QD heterostructures with two QD layers (d_2=5 nm). The structure parameters are similar to the QD samples studied in this paper and the effect of the InGaAs strain relaxation layer is neglected. The dependence of $\Delta R/R$ on d_1 is shown in Fig. 4 for different refractive index changes of Δn_2=0.1 and 0.2. It can be seen that for $d_1 \sim 100$ nm used in our samples, only a small negative differential reflection can be obtained. This feature is in good agreement with our experimental observations. Also, it indicates that an improvement in the differential reflection signal can be achieved by either increasing or decreasing d_1. In Fig. 3, it is also found that the time constant of the first stage is slightly larger in the p-doped QDs as compared to that in the undoped QDs. We think that the incorporation of the Be-doped GaAs layer into the GaAs cap layer is responsible for this behavior.

V. FITTING OF EXPERIMENTAL DATA AND EXTRACTION OF CAPTURE TIMES

Apparently, the differential reflection spectra of the QD samples can be fitted by two exponential decays with very short time constants and one exponential rise with a long time constant, i.e.,

$$\Delta R(t)/R \propto a + b(e^{-t/\tau_{b\text{-}w}} + e^{-t/\tau_{e,h}} - e^{-t/\tau_r}), \tag{6}$$

where $\tau_{b\text{-}w}$ and $\tau_{e\text{-}h}$ represent the carrier capture time from the barrier into the wetting layer and that from the wetting layer into the QDs, τ_r stands for the carrier recombination time in the QDs, and a and b are constants. Here, we do not discriminate the capture times of electrons and holes into the QDs because of two reasons. One is that the absorption and thus the reflection of the QDs will be modified once a kind of carrier (electron or hole) is captured into the QDs. This is clearly different from the time-resolved PL measurements where the presence of both carriers is necessary to generate PL signals. Therefore, the physical meaning of $\tau_{e\text{-}h}$ needs to be carefully identified. As will be shown later in Sec. VII, for the p-doped QDs, it may represent the capture time of either electrons or holes, depending on the pump power used in the measurements. The other reason is that there exists an InGaAs strain relaxation layer on top of the InAs QDs from which many carriers are captured into the QDs. Thus, the potential barrier existing for holes in the InAs wetting layer has less influence on the capture of holes.[4]

VI. DEPENDENCE OF CARRIER CAPTURE TIMES ON INJECTED CARRIER DENSITY

We have carried out pump-probe reflection measurements for the three samples under different pump powers in order to find out the influence of the injected carrier density on the carrier dynamics. Their differential reflection spectra obtained at different pump powers for the bulk GaAs, the undoped, and p-doped InAs/GaAs QDs are shown in Figs. 5(a)–5(c), respectively. Relying on the exponential fitting method described above, we are able to extract the time constants for carrier capture and recombination processes. Here, we are mainly concerned with the capture process that governs the operation speed of QD-based devices. In Figs. 6(a) and 6(b), we plot the two capture times ($\tau_{b\text{-}w}$ and $\tau_{e,h}$) as a function of the pump power, or equivalently the injected carrier density, for the undoped and p-doped QDs. For the undoped QDs, $\tau_{b\text{-}w}$ and $\tau_{e,h}$ are found to be $\sim$0.25 and $\sim$1.5 ps at low carrier densities. Therefore, it takes $\sim$1.75 ps to transfer the carriers from the GaAs barrier into the InAs QDs. This value is shorter than those previously reported.[21] We think that the introduction of the InGaAs strain relaxation layer may accelerate the carrier capture process. With increasing injected carrier density, we observe a gradual increase of $\tau_{b\text{-}w}$ to $\sim$0.7 ps and a slight decrease of $\tau_{e,h}$ to $\sim$1.4 ps. The increase of $\tau_{b\text{-}w}$ is similar to the slow down of the carrier thermalization at high excitation densities observed in the bulk GaAs. It is mainly caused by the state filling effect occurring in the InGaAs strain relaxation layer and the InAs wetting layer. A different carrier dynamical process is observed in the p-doped QDs. At low carrier den-

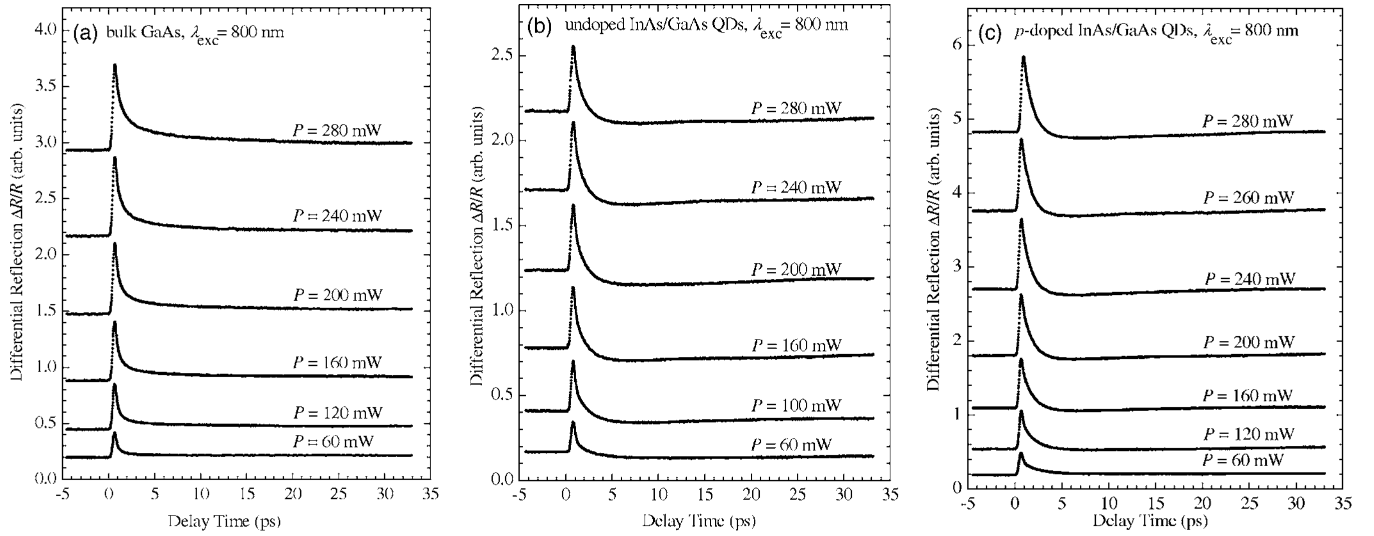

FIG. 5. Differential reflection spectra measured at different pump powers for (a) the bulk GaAs, (b) the undoped InAs/GaAs QDs, and (c) the *p*-doped InAs/GaAs QDs.

sities, $\tau_{b\text{-}w}$ is similar to that in the undoped sample, while $\tau_{e,h}$ is slightly larger. As carrier density is increased, we find a rapid decrease of $\tau_{e,h}$ and a fast rise of $\tau_{b\text{-}w}$ when the pump power is raised from 120 to 200 mW. Under high excitation densities, the value of $\tau_{e,h}$ becomes only half of that in the undoped QDs. These features are completely different from the previous observations in time-resolved PL measurements.[21] In the transient PL measurements, a threefold decrease of the carrier capture time was found in doped QDs and it did not exhibit any dependence on the injected carrier density. These "abnormal" behaviors found in the *p*-doped QDs will be discussed in the next section.

VII. DISCUSSION

Now let us discuss the carrier dynamics in the undoped and *p*-doped QDs derived from the pump-probe reflection measurements. For the sake of clarity, we schematically show the discrete energy levels in the conduction and valence bands of the undoped and *p*-doped QDs together with the initial carrier distributions on them in Figs. 7(a) and 7(b). As mentioned above, different from the generation of transient PL signals where the simultaneous presence of electrons and holes in the ground state is necessary, the occupation of the energy levels by only one kind of carriers will modify the absorption of the QD layer and thus its refractive index and reflection. For instance, the transition from E_{1h} to E_{1e} by absorbing an electron is allowed in the undoped QDs before the injection of carriers. Once an injected electron (or a hole) relaxes to E_{1e} (or E_{1h}), however, such a transition will be inhibited, resulting in a modification in the absorption of the QDs. Therefore, the reflection of the undoped QDs is changed once electrons or holes are captured from the wetting layer into the QDs. In general, the captured carriers first occupy the high-energy levels and then relax to the low-energy levels. Since the high-energy levels can accommodate many carriers, the modification of the absorption is not significant when they are occupied by a small number of carriers. In contrast, the occupation of the low-energy levels gives rise to a relatively large change in the absorption of the QDs. Hence, the time constant $\tau_{e,h}$ derived from the differential reflection spectra of the undoped QDs is the sum of the carrier capture and relaxation times. In addition, it should be the time constant for the faster carriers, i.e., electrons.

As for the *p*-doped QDs, the situation is completely dif-

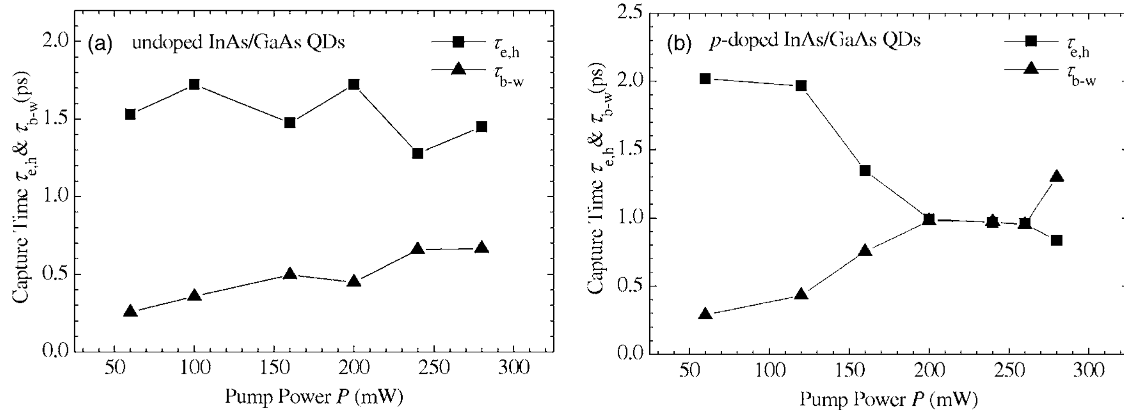

FIG. 6. Injected carrier density dependence of the carrier capture time from the GaAs barrier into the InAs wetting layer and that from the InAs wetting layer into the InAs QDs in (a) the undoped and (b) the *p*-doped InAs/GaAs QDs.

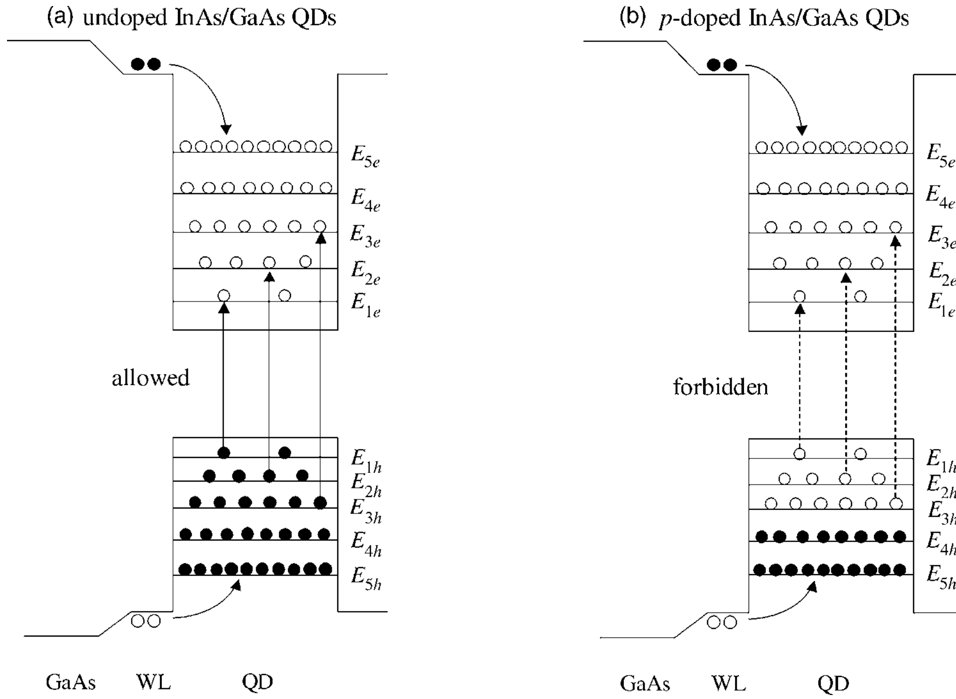

FIG. 7. Schematic of the electron and hole energy levels in the conduction and valence bands together with the carrier distribution in them. (a) The undoped InAs/GaAs QDs; (b) the *p*-doped InAs/GaAs QDs.

ferent due to the large built-in population of holes prior to the excitation. Since the low-energy levels in the valence band have already been occupied by holes, there is no modification of the absorption when electrons are captured into the low-energy levels of the conduction band, e.g., E_{1e}, E_{2e}, and E_{3e}. At low excitation densities, the average number of the generated electrons for each QD is not sufficient to fill the low-energy levels of the conduction band. Although the capture and relaxation of the electrons are very fast through the scattering with the built-in holes,[21] they are not reflected in the differential reflection spectra because the absorption of the QDs is not changed by these processes. In this case, only when the high-energy levels of the valence band (e.g., E_{4h} and E_{5h}) are occupied by the injected holes, the absorption of the QDs is changed. Therefore, the time constant derived from the differential reflection spectra represents the capture time of holes into the high-energy levels in the *p*-doped QDs. It is slightly longer than the capture and relaxation times of electrons into the low-energy levels in the undoped QDs. Thus, no information about the capture time of electrons can be extracted at low excitation densities. With increasing excitation power, the low-energy levels in the conduction band that do not induce any absorption change will eventually be filled by the generated electrons. Since the capture of electrons is much faster than that of holes due to the scattering with the built-in holes, the modification of the absorption in this case mainly arises from the occupation of the high-energy levels of the conduction band by the injected electrons (e.g., E_{4e} and E_{5e}). Thus, the time constant we derived from the differential reflection spectra represents the total time for electrons to occupy the high-energy levels. It includes the capture time of electrons into the low-energy levels and the time for electrons to sequentially fill from the low-energy levels to the high-energy ones. Its value is only half the capture time of holes into the high-energy levels, implying that the capture and relaxation of electrons into the low-energy levels is very fast in the *p*-doped QDs.

In fact, the filling of the low-energy levels in the conduction band with increasing excitation density is clearly reflected in Fig. 6(b). While no obvious change in the capture time is observed for pump powers lower than 120 mW, we find a rapid transition of the capture time from ~ 2 to ~ 1 ps when the pump power is increased to 200 mW. Due to the difference in carrier dynamics, the *p*-doped QDs need more injected carriers than the undoped QDs in order to achieve the same absorption change. Actually, we have seen in Figs. 3 and 5 that under the same excitation, the negative differential reflection induced in the *p*-doped QDs is always weaker than that in the undoped QDs. This is because the filling of the low-energy levels by the injected electrons do not contribute to the change in the absorption of the QDs. Therefore, our experimental observations are not contradictory to but are consistent with the results obtained by time-resolved PL measurements.[21]

VIII. SUMMARY

In summary, we have studied by FDTD simulations and theoretical calculations the dependence of the differential reflection signals on the structure parameters of QD heterostructures in pump-probe reflection measurements. Based on that, we have compared the ultrafast carrier dynamics in the undoped and *p*-doped InAs/GaAs QDs by utilizing the pump-probe reflection measurements. The carrier capture times from the GaAs barrier into the InAs wetting layer and those from the InAs wetting layer into the InAs QDs have been extracted by properly fitting the differential reflection spectra. In addition, the dependence of carrier dynamics on the injected carrier density has been clarified. It is found that for the *p*-doped QDs, the time constant of the second decay represents the capture time of holes at low carrier densities,

while it gives the capture and relaxation times for electrons at high carrier densities. The built-in population of holes in the *p*-doped QDs plays a crucial role in determining the carrier dynamics, and it may be beneficial to the performance of QD-based devices.

ACKNOWLEDGMENTS

The authors acknowledge the financial support from the National Natural Science Foundation of China (Grant No. 10674051), the Natural Science Foundation of Guangdong province of China (Grant No. 06025082), and the Program for Innovative Research Team of the Higher Education in Guangdong (Grant No 06CXTD005). One of the authors (S. Lan) would like to thank the financial support by the Program for New Century Excellent Talents (NCET) in University of China.

[1]Y. Arakawa and H. Sakaki, Appl. Phys. Lett. **40**, 939 (1982).
[2]D. Bimberg, M. Grundmann, and N. N. Ledentsov, *Quantum Dot Heterostructures* (Wiley, Chichester, 1999).
[3]R. Ferreira and G. Bastard, Appl. Phys. Lett. **74**, 2818 (1999).
[4]D. A. Yarotski, R. D. Averitt, N. Negre, S. A. Crooker, A. J. Taylor, G. P. Donati, A. Stintz, L. F. Lester, and K. J. Malloy, J. Opt. Soc. Am. B **19**, 1480 (2002).
[5]D. Morris, N. Perret, and S. Fafard, Appl. Phys. Lett. **75**, 3593 (1999).
[6]I. Magnusdottir, A. V. Uskov, S. Bischoff, B. Tromborg, and J. Mørk, J. Appl. Phys. **92**, 5982 (2006).
[7]J. Feldmann, S. T. Cundiff, M. Arzberger, G. Böhm, and G. Abstreiter, J. Appl. Phys. **89**, 1180 (2001).
[8]T. S. Sosnowski, T. B. Norris, H. Jiang, J. Singh, K. Kamath, and P. Bhattacharya, Phys. Rev. B **57**, R9423 (1998).
[9]B. Ohnesorge, M. Albrecht, J. Oshinowo, A. Forchel, and Y. Arakawa, Phys. Rev. B **54**, 11532 (1996).
[10]E. W. Bogaart, J. E. M. Haverkort, T. Mano, T. van Lippen, R. Nötzel, and J. H. Wolter, Phys. Rev. B **72**, 195301 (2005).
[11]E. A. Zibik, L. R. Wilson, R. P. Green, G. Bastard, R. Ferreira, P. J. Phillips, D. A. Carder, J.-P. R. Wells, J. W. Cockburn, M. S. Skolnick, M. J. Steer, and M. Hopkinson, Phys. Rev. B **70**, 161305(R) (2004).
[12]A. V. Uskov, F. Adler, H. Schweizer, and M. H. Pilkuhn, J. Appl. Phys. **81**, 7895 (1997).
[13]F. Adler, M. Geiger, A. Bauknecht, F. Scholz, H. Schweizer, M. H. Pilkuhn, B. Ohnesorge, and A. Forchel, J. Appl. Phys. **80**, 4019 (1996).
[14]P. D. Buckle, P. Dawson, S. A. Hall, X. Chen, M. J. Steer, D. J. Mowbray, M. S. Skolnick, and M. Hopkinson, J. Appl. Phys. **86**, 2555 (1999).
[15]P. Borri, S. Schneider, W. Langbein, U. Woggon, A. E. Zhukov, V. M. Ustinov, N. N. Ledentsov, Zh. I. Alferov, D. Ouyang, and D. Bimberg, Appl. Phys. Lett. **79**, 2633 (2001).
[16]U. Bockelmann and G. Bastard, Phys. Rev. B **42**, 8947 (1990).
[17]X.-Q. Li, H. Nakayama, and Y. Arakawa, Phys. Rev. B **59**, 5069 (1999).
[18]H. Benisty, C. M. Sotomayor-Torrès, and C. Weisbuch, Phys. Rev. B **44**, 10945 (1991).
[19]T. Inoshita and H. Sakaki, Phys. Rev. B **46**, 7260 (1992).
[20]E. Towe and D. Pan, IEEE J. Sel. Top. Quantum Electron. **6**, 408 (2000).
[21]K. Gündoğdu, K. C. Hall, T. F. Boggess, D. G. Deppe, and O. B. Shchekin, Appl. Phys. Lett. **85**, 4570 (2004).
[22]K. W. Sun, A. Kechiantz, B. C. Lee, and C. P. Lee, Appl. Phys. Lett. **88**, 163117 (2006).
[23]O. B. Shchekin and D. G. Deppe, Appl. Phys. Lett. **80**, 2758 (2002).
[24]S. Sauvage, P. Boucaud, F. Glotin, R. Prazeres, J.-M. Ortega, A. Lemaître, J.-M. Gérard, and V. Thierry-Flieg, Appl. Phys. Lett. **73**, 3818 (1998).
[25]J. I. Lee, J.-Y. Leem, and H. G. Lee, Physica E (Amsterdam) **15**, 94 (2002).
[26]J. Siegert, S. Marcinkevičius, and Q. X. Zhao, Phys. Rev. B **72**, 085316 (2005).
[27]V. Cesari, W. Langbein, P. Borri, M. Rossetti, A. Fiore, S. Mikhrin, I. Krestnikov, and A. Kovsh, Appl. Phys. Lett. **90**, 201103 (2007).
[28]Z. L. Yuan, E. R. A. D. Foo, J. F. Ryan, D. J. Mowbray, M. S. Skolnick, and M. Hopkinson, Physica B **272**, 12 (1999).
[29]K. W. Sun, J. W. Chen, B. C. Lee, C. P. Lee, and A. M. Kechiantz, Nanotechnology **16**, 1530 (2005).
[30]S. Marcinkevičius and R. Leon, Phys. Rev. B **59**, 4630 (1999).
[31]S. Marcinkevičius and R. Leon, Appl. Phys. Lett. **76**, 2406 (2000).
[32]T. Piwonski, I. O'Driscoll, J. Houlihan, G. Huyet, R. J. Manning, and A. V. Uskov, Appl. Phys. Lett. **90**, 122108 (2007).
[33]Q. Li, Z. Y. Xu, and W. K. Ge, Solid State Commun. **115**, 105 (2000).
[34]B. Liu, Q. Li, Z. Xu, and W. K. Ge, J. Phys.: Condens. Matter **13**, 3923 (2001).
[35]K. S. Yee, IEEE Trans. Antennas Propag. **AP-14**, 302 (1966); in this article, a commercially available software developed by Rsoft Design Group (http://www.rsoftdesign.com) is used for the numerical simulations.
[36]D. Leonard, K. Pond, and P. M. Petroff, Phys. Rev. B **50**, 11687 (1994).
[37]B. R. Bennett, R. A. Soref, and J. A. D. Alamo, IEEE J. Quantum Electron. **26**, 113 (1990).
[38]For the refractive indices of GaAs and InAs at 800 nm, please refer to D. E. Aspnes, and A. A. Studna, Phys. Rev. B **27**, 985 (1983).
[39]Z. Knittl, *Optics of Thin Films* (Wiley, London, 1976).
[40]M. Born and E. Wolf, *Principles of Optics*, 5th ed. (Pergamon, Oxford, 1975).
[41]S. J. Pearton, J. C. Zolper, R. J. Shul, and F. Ren, J. Appl. Phys. **86**, 1 (1999).